



ELSEVIER

Applied Acoustics 56 (1999) 1–24

**applied  
acoustics**

# Scattering by a barrier in a room

D. Ouis

*Department of Engineering Acoustics, Lund Institute of Technology, PO Box 118,  
S-221 00LundSweden*

Received 23 June 1997; received in revised form 18 February 1998; accepted 9 March 1998

---

## Abstract

In this paper, the prediction of the effect of a simple scattering element on the acoustics of a room is studied. For the sake of simplicity, the room is a rectangular one with hard walls, and the scattering element is a horizontal thin hard strip-like barrier placed at one or two side walls. The diffraction model adopted for the sharp edge of the scattering hard strip is an exact one based on geometrical optics assumptions. The impulse response of the room may be predicted through using the image sources method for the specular reflections at the hard walls and the barrier in combination with the diffraction model which is expressed in the time domain. From the impulse response many room acoustical parameters related to the subjective rating of the room can be processed. Among these, the inter-aural cross-correlation coefficient (IACC) between two space separated impulse responses (these are usually measured at the ear entrances of a listener), which is a measure of the diffuseness of the field, can thus be calculated at different positions in the room. Another factor, the early lateral energy fraction (ELEF) can also be calculated. Some experimental results on the measurement of the impulse response and of the IACC on a scale model are also presented to support the theoretical ones. © 1998 Elsevier Science Ltd. All rights reserved.

*Keywords:* Scattering; barrier; Room acoustics; IACC; Early lateral energy fraction.

---

## 1. Introduction

One of the most outstanding questions facing the architectural acoustician in his design to a listening space is to foresee the overall sound quality in the space before its building achievement. The reverberation time, believed for a long time as being the only parameter of decisive importance for the propagation of sound in a closed space is still determined by using relatively simple formulas. Although the reverberation time has attracted the interest of many workers in the field of acoustics so that Sabine's formula:

$$T = \frac{0.16V}{\sum_i a_i S_i} \quad (1)$$

has got some better refinements during the years, it is a well known fact nowadays that the reverberation time is one but not the only one factor upon which good listening conditions rely [1]. The fact that rooms with equal reverberation times could sound very much unlike laid the ground for further investigations of objective room quantities that could be closely related to the human listening impressions. Over almost three decades of time extending from the early 1950s to the 1970s there has been a landing of many such parameters in the attempt to fill the gap between designing a hall and enjoying listening in it. Most of the formulas defining these parameters are semi-empirical based on the experiment of their own authors or on the results of extensive listening tests. These parameters were subject of improvements in their form and simplicity along the years. Moreover, some parameters have got more than one formulation making by this a larger application area depending on one's conviction.

To restrict ourselves to a single example, we take the case of the inter aural cross-correlation coefficient (IACC) [2]. Keet in 1968 found that the IACC is related to the apparent source width. In 1974 it was found by Schroeder and his co-workers that the IACC is one of three important factors in listening impressions while Ando in 1985 concludes in his experiments that the IACC was among four important uncorrelated factors. Six years later Hidaka conjectured that two separate values of IACC are to be distinguished; one for early sound energy, determined over the first 80 ms of the impulse response and which is better correlated to spatial impression (SI), and one for late sound energy calculated in the range between 80 ms and 3 s and which gives a measure of the feeling of envelopment. Moreover, this last author gives a recommendation about the measurement positions with the use of a standardised dummy head, the source of the signal and its positions on the stage in order to present average values and, he further suggests a “scale of importance in hearing” to make a sort of standard definition of the IACC. Regarding the definition of the IACC, different authors give it different forms. Cremer, in 1976, found it reasonable to call the absolute value of the coefficient:

$$\kappa(\tau) = \frac{\int_0^{\infty} p_l(t)p_r(t+\tau)dt}{\left[ \int_0^{\infty} p_l^2(t)dt \int_0^{\infty} p_r^2(t)dt \right]^{\frac{1}{2}}} \quad (2)$$

“Inter-aural cross-correlation coefficient” ( $p_l$  and  $p_r$  being, respectively the pressures measured at the left and right ears of a dummy head) [1]. Damaske recommended the maximum of  $|\kappa|$  as a room acoustical criterion and Keet proposed instead of infinity, a limited time  $t_g$  for the integration, giving hence a new “short time correlation coefficient” after evaluation at  $\tau = 0$ . Gottlob on the other hand preferred to use the maximum of  $|\kappa|$  for  $t_g = 50$  ms with the further restriction that  $\tau = 1$  ms.

This last definition is the one Kuttruff opted for with the slight change that  $t_g$  be taken 80 ms instead of 50 ms [3]. Finally, Ando chooses the concept of long time IACC defined in a similar way as in Eq. (2) with the exception that the integrations be performed in the interval  $[-35\text{ s}, 35\text{ s}]$  [4]. This short overview on the history of the IACC gives an idea about how rich discussions can rise and large literature written when investigating psychological implications of changes in physical room acoustical quantities.

## 2. Theory

The starting point for the determination of the sound field in a closed space is the consideration of the wave equation:

$$\Delta p - \frac{1}{c^2} \frac{\partial^2 p}{\partial t^2} = 0 \quad (3)$$

where  $p$  is the pressure,  $c$  the velocity of propagation of sound waves in the fluid filling the closed space and  $\Delta$  the three-dimensional Laplace operator. The solution of this equation needs the knowledge of the conditions satisfied by either the pressure or the particle velocity (or a combination of both in the form of a wall impedance) at the boundaries of the closed space. As long as the frequency is so low that the peaks in the frequency response of the room are well separated from each other, the problem of the room excited by a sound source is most adequately solved by a standing wave analysis. However, when the frequency gets higher, so that two successive response peaks can no longer be easily separated in the frequency response of the room, then the problem is attacked by geometrical or statistical room acoustics. The point of departure between the two methods is at the so-called Schröder's frequency  $f_g$ :

$$f_g \cong 2000\sqrt{T/V} \text{ Hz} \quad (4)$$

where  $T$  is the reverberation time in seconds and  $V$  the volume of the room in  $\text{m}^3$ . In typical rooms, the modal density, that is the number of eigenmodes per unit frequency, increases as the square of the frequency and one can thus see what a hard task it is to formulate the room response at higher frequencies by means of eigenmode expansion. In geometrical room acoustics, waves are replaced by rays and if the frequency is enough high (a condition usually satisfied above 1 kHz for practical cases) the wavelength becomes so short that the reflecting surfaces can be assumed as infinitely large and consequently wave reflections can be dealt with by the mirror images method.

### 2.1. The image sources method

When considering the solution of problems arising in room acoustics, two algorithms are in general of wide acceptance to simulate the response of a room in which

a sound source is activated. The image sources method and the particle ray method. These two methods have been the subject of interest of acousticians for several decades and their merits are most often discussed in terms of both computing time and memory storage when they are to be run on computers [5]. In the special case of rectangular rooms the image sources method is by far easier and better implemented in computer programs than the ray method [5–7].

## 2.2. Knife edge diffraction model

The simplest example that one can think of in diffraction theory is that of determining the field around a half plane on which impinges a plane wave under some incidence angle  $\theta_0$  (Fig. 1). This problem is treated in two dimensions if one further makes the assumption that the wave vector of the falling wave is perpendicular to the edge of the half plane. For a long time ago, it was a clear fact that the field at some point of this configuration is not the one predicted by geometrical assumptions, i.e. the interference of a direct field and the one due to the eventual image of the source through the half plane. A third wave originating at the knife edge was believed to ensure the progressive transition from the insonified to the uninsonified sides of space.

Setting the problem mathematically is to solve the wave equation with the appropriate boundary conditions on the half plane. For many decades, this “simplest” problem kept without any satisfactory solution until at the shift of the century, Sommerfeld presented, the first, the exact solution (see for instance [8]). Now, this solution involves special mathematical artifices, and to separate the field

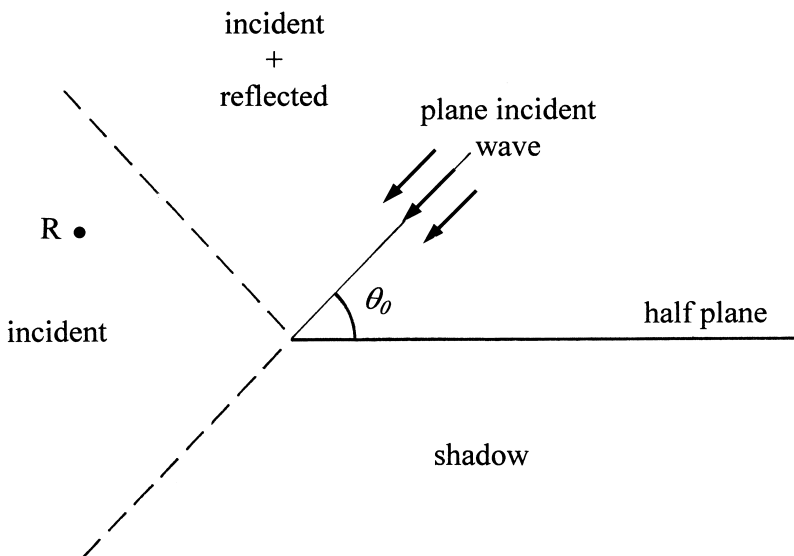


Fig. 1. A half plane on which a plane wave falls normally at an angle  $\theta_0$ .

into its three different components, the direct, the reflected and the diffracted waves, requires one to be at quite high frequencies.

Since Sommerfeld’s landmark work, many attempts were made to join between the exactness of the diffraction theory and the flexibility of geometrical optics. Among these, the popular geometrical theory of diffraction (GTD) was subject of successive perfections during almost two decades of time and has been used as a tool for solving many diffraction problems arising in electromagnetism and acoustics [9,10]. All these last named methods share the common property of expressing the field quantities in the frequency domain as a consequence of solving the wave equation under steady state conditions.

As in our case one is merely interested in studying the time evolution of the field quantities, another approach is thus preferred. Hence, considering in Fig. 2 the problem of diffraction by a hard wedge of exterior angle  $\theta_w$  and subtending a fluid of density  $\rho$ , then, if the point source S with strength  $S$  radiates a Dirac pressure pulse of amplitude:

$$p(t) = \frac{\rho S}{4\pi R} \delta\left(t - \frac{R}{c}\right) \tag{5}$$

where  $R$  is the distance range, then the receiver point R would, more than the possibility of detecting the direct pulse and its reflection on one or both sides of wedge, it would receive a disturbance  $p_d(t)$  diffracted by the tip of the wedge at a time  $\tau_0$

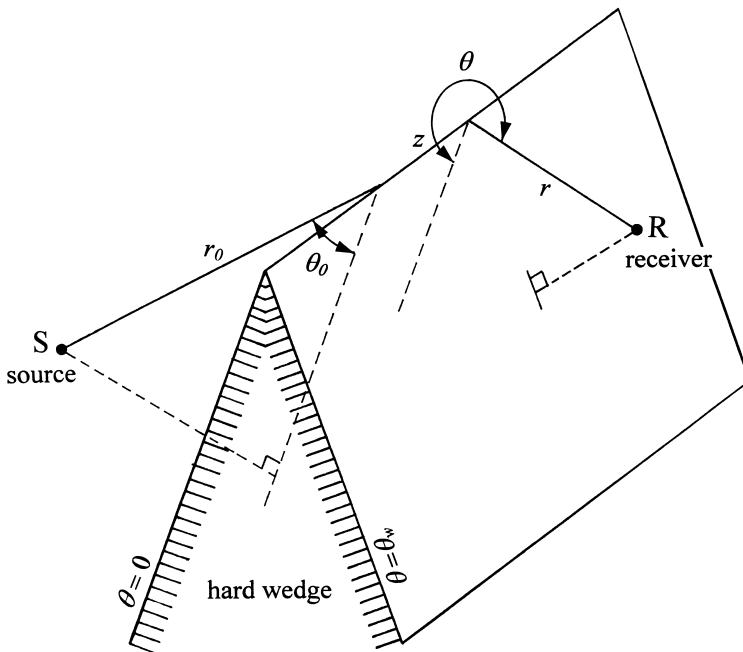


Fig. 2. The hard wedge with exterior angle  $\theta_w$ . S is the point source and R the receiver.

(called the least time, for the shortest travel distance from source to receiver over the wedge) after the emission of the pulse from S: [11,12]

$$\tau_0 = [(r + r_0)^2 + z^2]^{\frac{1}{2}}/c \quad (6)$$

The diffracted field  $p_d(t)$  is then expressed as:

$$p_d(t) = \frac{-S\rho c}{4\pi\theta_w} \{\beta\} \frac{\exp(-vy)}{rr_0 \sinh(y)} \quad (7)$$

where  $v$  is the wedge index defined as:

$$v = \pi/\theta_w \quad (8)$$

$\{\beta\}$  is the sum of four terms resulting from the different combinations of the signs in:

$$\{\beta\} = \frac{\sin[v(\pi \pm \theta \pm \theta_0)]}{1 - 2 \exp(-vy) \cos[v(\pi \pm \theta \pm \theta_0)] + \exp(-2vy)} \quad (9)$$

and:

$$y = \operatorname{arccosh}\left(\frac{c^2 t^2 - (r^2 + r_0^2 + z^2)}{2rr_0}\right) \quad (10)$$

To formulate expression (7) in the frequency domain requires a Fourier transformation which, to the best of our knowledge is not available in an explicit closed form. Instead, the problem is contoured in another way. Most of the energy of the disturbance given by Eq. (7) arrives just after the least time  $\tau_0$ . Hence, the idea is to approximate this expression at a time  $t$  near  $\tau_0$ , perform its exact Fourier transform and then digital Fourier transform (DFT) the difference between the exact and the near- $\tau_0$  fields [12].

### 2.3. Application to the case of the rectangular room with a thin barrier

As discussed earlier, the image sources method suits best the acoustical simulation of rectangular rooms. In this part, we shall present its implementation in combination with the diffraction model to the rectangular room with the thin barrier at a wall. In the figure below, a room of size width  $\times$  length  $\times$  height =  $X \times Y \times Z$  is represented with only its four side walls. The coordinates of the mirror sources through the walls may be expressed as:

$$\pm x_s \pm 2lX; \quad \pm y_s \pm 2mY; \quad z_s \quad (11)$$

where the source S is supposed having the coordinates  $(x_s, y_s, z_s)$  and  $(l, m)$  is a couple of integer numbers including 0.

In the room without the barrier in its place, the receiver sees all the image sources through the side walls (Fig. 3), but once the barrier is settled at its place, then visibility tests must be run for the mirror sources (MSs) to account for their visibility through the barrier or any of its images.

Another test is also necessary in order to take into account the possibility that the barrier or any of its images could mask a MS that was visible prior to mounting the barrier. When one goes one step further in complexity by setting a ceiling on the four sided room, then in principle, the visibility testing of the mirror sources is the same:

- The receiver should not see the source or its wall images through the barrier or any of the barrier's images.
- The receiver should not see the source images mirrored by the ceiling through any of the barrier or the barrier's images.
- For the wall images of the source mirrored through the barrier, the receiver should see them through the barrier or its wall images.

Cases (a) and (b) are illustrated in Fig. 4.

In this figure, the line joining some virtual source to the receiver is sectioned every time it crosses a real or image reflecting surface. Starting from the receiver, and after the (real) segment of the line between the receiver and the first (real) reflecting surface, every resulting segment is mirrored through the reflecting surface it crossed first. This procedure is made to bring all the reflections in the real room, simulating thereby the real trajectory of the ray. If the last extremity of the last segment falls on

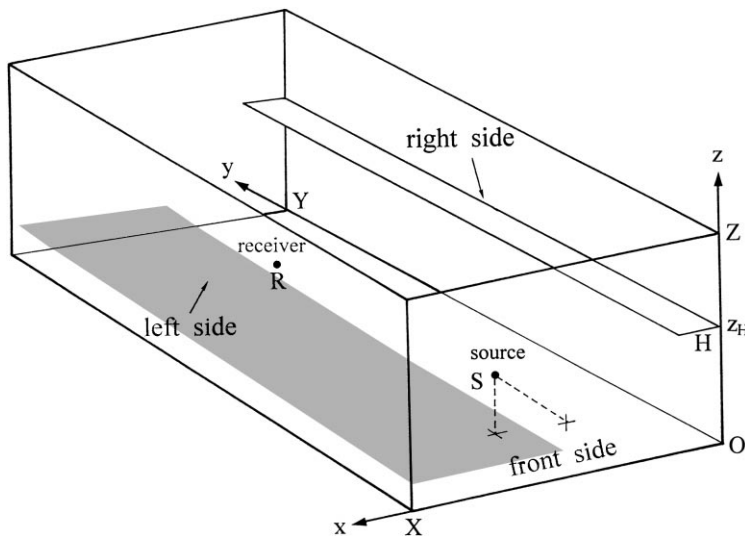


Fig. 3. A four hard walls room with on its right side wall and at a height  $z_H$  a thin hard horizontal barrier of width  $H$ . The grayed area is the region of existence of the geometrical doubly specular reflection by the barrier on the right wall.

the real source then the virtual source is visible otherwise it is thrown in a sort of waste basket.

We content ourselves by treating the rectangular room with perfectly absorbing floor as a study example of a full seated hall where the combination audience–floor presents a quite high degree of absorption especially in the mid-auditory frequency range.

As a typical case study, we take a shoe box shaped room of size length  $\times$  width  $\times$  height =  $25 \times 15 \times 10 \text{ m}^3$ , where a 1.5 m wide thin hard barrier is settled parallel to the floor at a height of 5.5 m on either one or two opposite side walls. The barrier is considered as a primary crude representation of a side balcony.

First, the impulse response of the room is calculated for an excitation by a triangular pulse. As one is interested only in the early contributions of the reflections, the study of the impulse response is confined to its first 100 ms. The excitation signal is shown in Fig. 5, both in the time and the frequency domains.

The program for these calculations was written in FORTRAN and along with processing the impulse response, it gives information on:

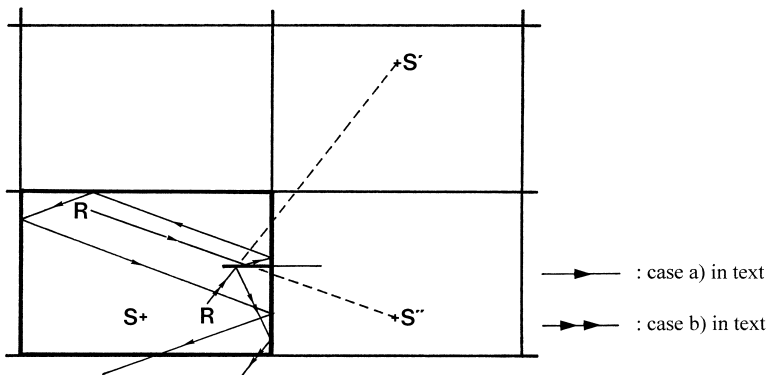


Fig. 4. Visibility of different image sources.

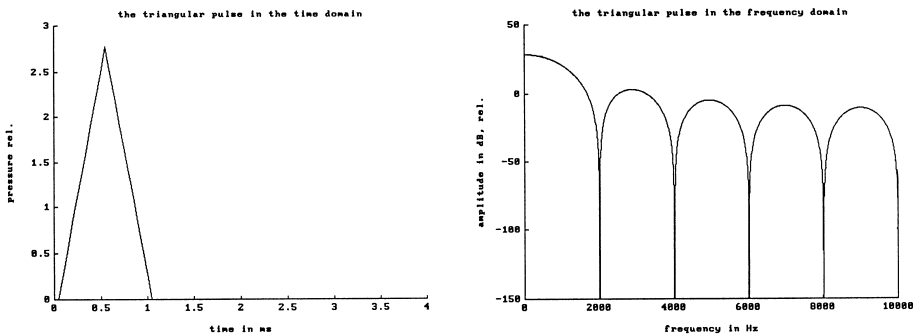


Fig. 5. The triangular excitation signal: left: time domain, sampling with  $\Delta t = 50 \mu\text{s}$ ; right: frequency domain.

- the arrival time of the direct (first) pulse to start the calculations on the impulse response at the suitable time;
- the number of visible and non-visible image sources through the walls and through the barrier;
- it calculates the early lateral energy fraction, ELEF, as defined by: [13]

$$ELEF = \frac{\int_0^{80 \text{ ms}} p_L^2(t) dt}{\int_0^{80 \text{ ms}} p^2(t) dt} \quad (12)$$

where  $p_L^2(t) = p^2(t) |\cos \theta|$ ,  $\theta$  being the incidence angle of the incoming pulse and the line normal to the median of the listener's head, and  $p$  the pressure;

- the inter-aural cross-correlation coefficient (IACC) as defined by: [3]

$$IACC = \text{maximum of } \varphi_{lr}(\tau), \quad |\tau| < 1 \text{ ms} \quad (13)$$

$$\varphi(\tau) = \frac{\int_0^{100 \text{ ms}} p_l(t) \cdot p_r(t + \tau) dt}{\left[ \int_0^{100 \text{ ms}} p_l^2(t) dt \cdot \int_0^{100 \text{ ms}} p_r^2(t) dt \right]^{\frac{1}{2}}} \quad (14)$$

where  $p_r$  and  $p_l$  are, respectively, the pressures at the right and left ears of the listener.

A block diagram for calculations on an ideal impulse response is shown in Fig. 6. Later on, some results will be presented for the filtered impulse responses, this would consequently affect slightly the block diagram by calculating the middle impulse response for a filtered excitation impulse, hence, giving the right contribution to the ELEF from the beginning. For the IACC, the right and left impulse responses are to be calculated for the unfiltered pulse until the stage of cross correlation where, for instance, they should be correlated with the time representation of the appropriate filter.

To see the effect of adding a simple scattering element in a room on the above mentioned parameters, calculations were carried out for a bare room, the same room with one horizontal hard barrier extending over the whole of its longest side wall, and for the same room with two similar such barriers symmetrically positioned on two opposite side walls. The same study was carried out for examining the effect of different frequency filterings of the impulse response.

### 2.3.1. Barrier and frequency effects on IACC and ELEF

In this part, a theoretical prediction of the frequency effects on the psychoacoustics of a room are presented. The calculations based on the algorithm of Fig. 6 are applied to a rectangular room with no supposed floor. The IACC and ELEF coefficients are elaborated from the filtered impulse response where the working cutoff is

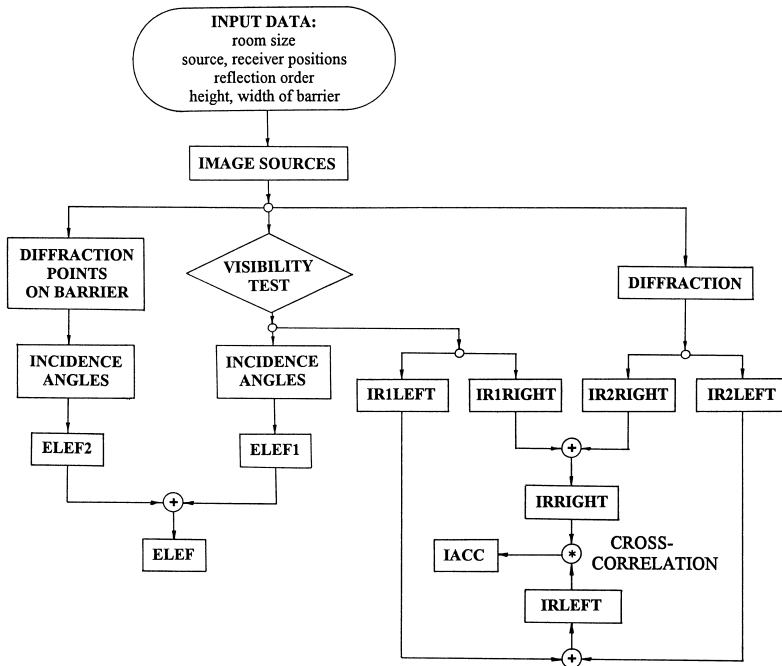


Fig. 6. Block diagram for the program to calculate the IACC and the ELEF coefficients in a room.

settled at 300 Hz. This frequency is chosen for the fact that many extensive psycho-tests on hearing under different frequency conditions have led to that the low frequency components of the test stimulus play a decisive role in the spatial impression (SI), with a special emphasis on frequencies around 300 Hz [4]. Therefore, three filters, a low pass, an octave band and a high pass at 300 Hz were applied to the impulse response of the room, respectively, without barrier, with one and with two barriers, to study the relative change in the values of the IACC and ELEF coefficients. The sound source  $S$  is settled in the median plane of the enclosure 4 m from the front wall and at a height of 2.5 m from the plane of the floor, or using the coordinates system of Fig. 3,  $S(7.5, 4.0, 2.5)$ . In the following, all calculations are made for this position of the sound source, hence, its mentioning as well as that of the height of the receiver at 1.2 m will be omitted throughout.

With regard to the bare room, the IACC as opposite to the ELEF, seems to exhibit a behaviour more dependent on the frequency. For a wide band excitation, its values are evenly distributed in the room with a sensible increment towards the rear of the room for the low frequencies. The region around the source is marked by a relatively high value of the IACC which broadens and flattens as a function of the pulse's bandwidth. The effect of adding side barriers in the room seems to be of a complicated character. Adding a single barrier (on the right side in the figures) breaks evidently the symmetry of the room, hence the distribution of the values of the acoustical objective parameters, but the effect of more barriers seems not to be

of a simple additive one at least for the ELEF. The addition of a single side barrier to the bare room has a desirable effect for the listener's positions in the half floor opposite the wall containing the barrier, where the IACC decreases in the front part of the room whereas the ELEF increases towards the rear. In the space near the mid plane of the room, the ELEF decreases relatively by about 15% while it remains almost unchanged in the space under the barrier. When a second barrier is settled opposite to the first one, its effect on the IACC appears to be additive to that of the first one, keeping hence unchanged the values in the room's mid space. At position lines parallel the barriers, the ELEF as opposite to the IACC decreases slightly. At last, one can mention that the HF components of the signal are more affected by the barrier(s) than the LF which is logically the result of using the image sources method. This trend is less marked for the ELEF. These results are summarised in Fig. 7 for the IACC and in Fig. 8 for the ELEF.

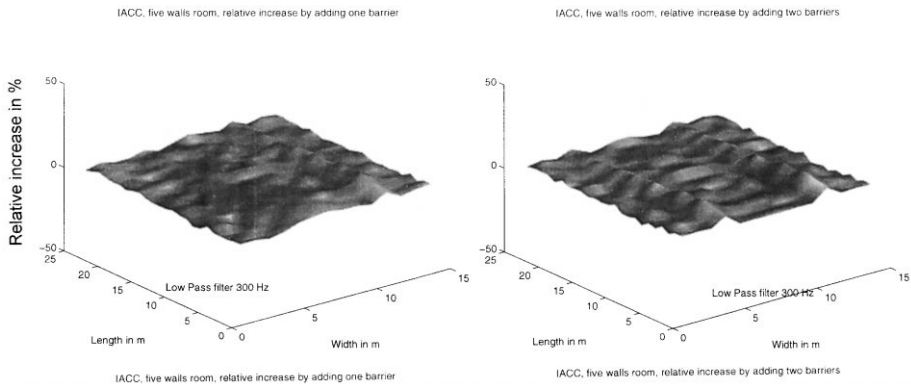


Fig. 7. Relative increment of IACC for a hard room without floor by adding one side barrier, left, and two barriers, right. Low pass filtering at 300 Hz.

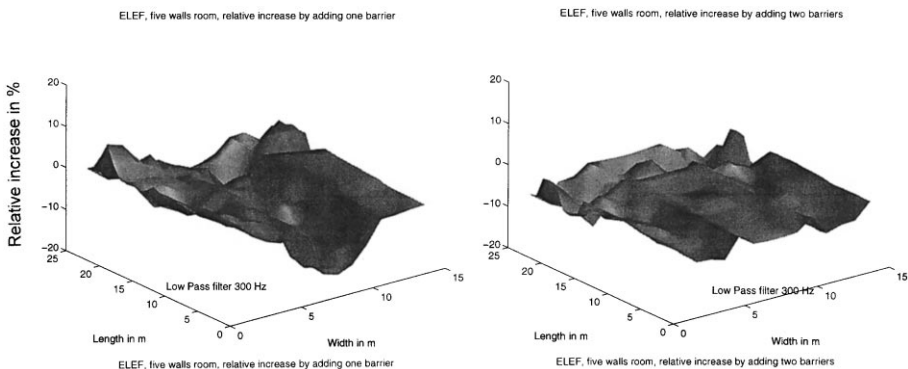


Fig. 8. Relative increment of ELEF for a hard room without floor by adding one side barrier, left, and two barriers, right. Low pass filtering at 300 Hz.

### 2.3.2. Effect of ceiling and floor

The addition of a ceiling and a floor to a room made of only the four side walls has for a consequence to distribute evenly the values of ELEF in the room. The IACC increases towards the back of the room at the low frequency range and shows a marked top near the sound source for higher frequencies. In general, adding one more reflecting surface to the four sided room increases the ELEF around the source and decreases it slightly elsewhere. Adding the other reflecting surface has a less noticeable effect on this coefficient. This trend is also found for the IACC for which the extra reflecting surfaces lower its values at the front of the enclosure and increase them at the back, especially at higher frequencies. If the unfavourable positions near the source and the walls are excluded, the floor and ceiling have opposite effects on the IACC and ELEF values. These cases are illustrated in Figs. 9 and 10.

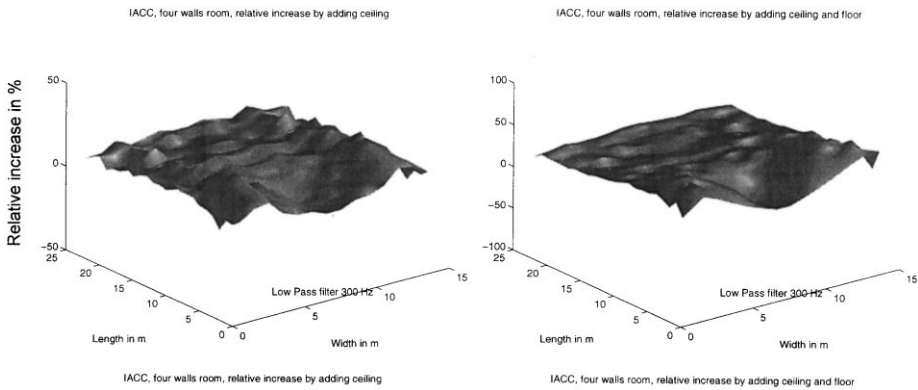


Fig. 9. Relative increment of IACC for a four hard walls room by setting a ceiling, left, and a ceiling and a floor, right. Low pass filtering at 300 Hz.

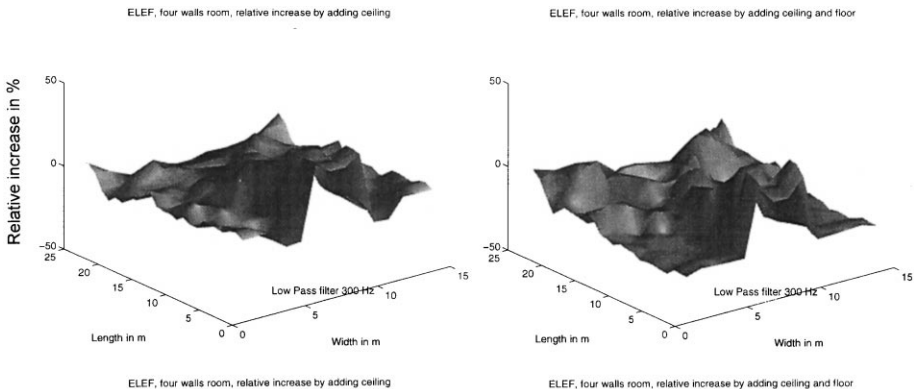


Fig. 10. Relative increment of ELEF for a four hard walls room by setting a ceiling: left, and a ceiling and a floor: right. Low pass filtering at 300 Hz.

2.3.3. *IACC and ELEF as function of the barrier width*

The results of the calculations of the IACC and ELEF are presented for the room comprising five hard walls as function of the width of two similar side barriers. These results are for the low pass filtered impulse response and the average of the values for six different positions in the room is taken.

From Fig. 11 one notices that the average IACC does not vary appreciably by changing the barrier width. On the other hand, the ELEF diminishes slightly for a barrier width equal approximately to 1/10 of the room width; the relative decrease is of the order of 10%.

2.3.4. *Optimization of barrier width as function of the room width*

An attempt was made here towards finding the optimum width of a single side barrier in a floorless room by maximising the ELEF or minimising the IACC as a function of the room width. The barrier is at a fixed height and the receiver is at some non extreme position in the room. The calculations are made for the low pass filtered response and the results are presented in Fig. 12.

It appears at first sight that the optimised width of the barrier increases linearly with the width of the room. This linearity is translated by a rather simple relationship between the widths of the barrier  $H$  and that of the room  $Y$  and is of the form:

$$H = Y/4 \tag{15}$$

This simple relationship works for both ELEF and IACC for a room having a width less than half its length, persists somehow for wider rooms in the case of the ELEF but breaks for the IACC.

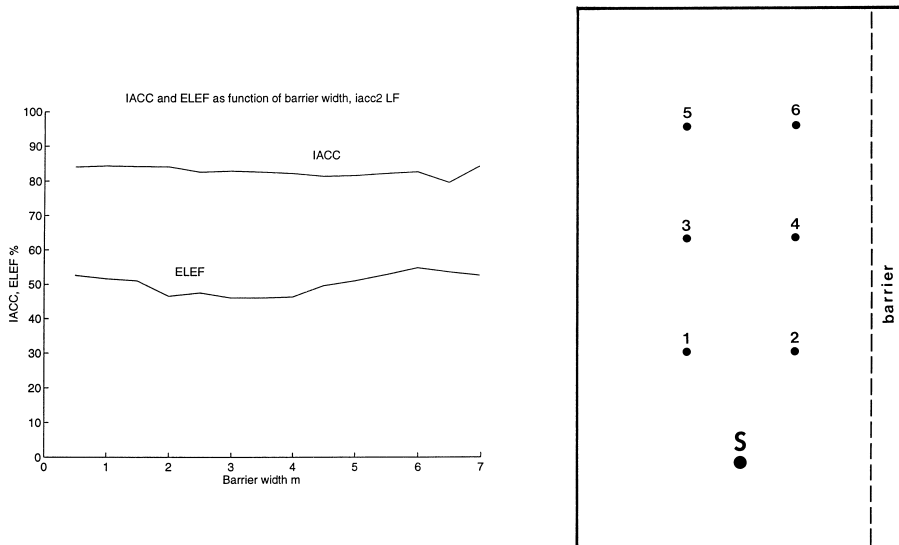


Fig. 11. IACC and ELEF vs barrier width in a floorless room, low pass filtering at 300 Hz. Average values taken for the six positions shown in the right portion.

### 2.3.5. IACC vs ELEF

The data for the IACC and ELEF coefficients relative to the floorless hard room are plotted in a diagram representing the ELEF as function of the IACC. This is illustrated in Fig. 13 where each point represents some position in the room. Depending on the frequency content of the impulse response, it looks as if the values of the IACC spread out more for shorter bandwidth filtering (BP in Fig. 13). For high

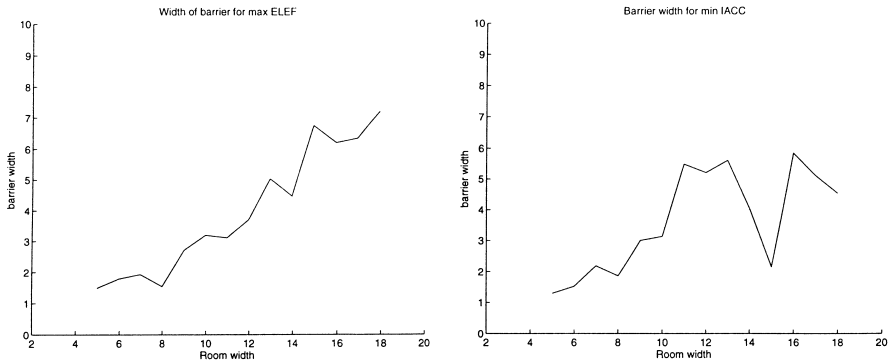


Fig. 12. Barrier width in a floorless hard room for: (left) maximisation of ELEF; and (right) minimization of IACC as function of the room width.

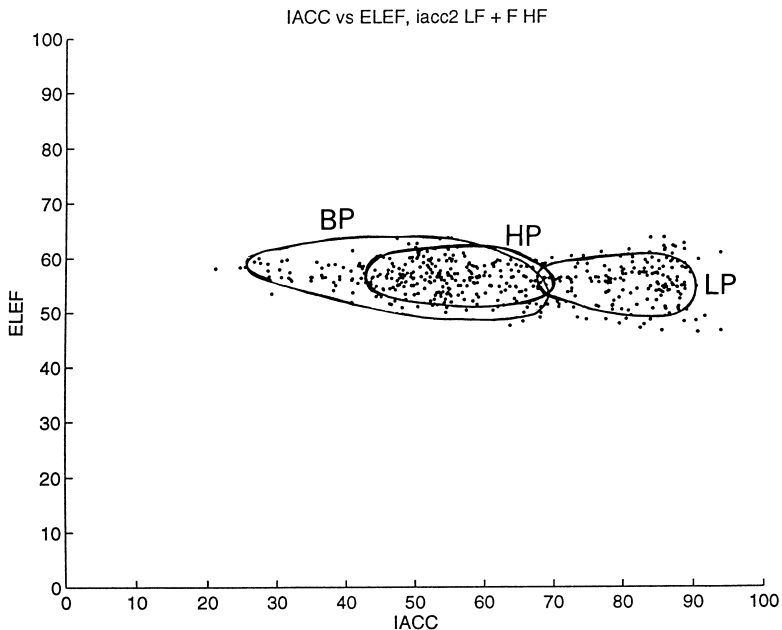


Fig. 13. IACC vs ELEF for a floorless hard room. LP: Low Pass, BP: Band Pass and HP: High Pass, all relative to 300 Hz.

pass filtering (HP), the IACC exhibits most of its values around 55% and all values are higher than about 45% while for low pass filtering (LP) the data points for ELEF cluster around 55% and IACC takes values in excess of 60%. This feature of the IACC vs the ELEF coefficients is also found for the cases of a room with or without ceiling and floor. Unfortunately, a simple relationship between these two coefficients could not be established easily. This could be attributed to the extreme case studied of the hard room, its geometrical regularity and/or the type of signal used for the calculations. This question is however left open and to be confirmed only by a more thorough study.

### 3. Experiment

Many of the room acoustical experiments are made on scale models, and often, the achievement of a large listening space is preceded by a thorough investigation of its performances on a reduced model. This allows for easiness and larger flexibility in varying the factors that have a direct effect on the acoustics of the real enclosure, such as absorption vs reverberation time or scattering elements vs field diffuseness to name some. However, some precautions are to be taken into account among which the most important is the frequency scaling factor  $s$  which is the scale of the model room to the real one. The factor  $s$  relates the frequency  $f_r$  on the real model to the frequency  $f_s$  on the scaled one by the simple relation: [1]

$$f_s = f_r/s \tag{16}$$

which leads to an expansion and shifting of the real audio frequency range of interest towards the ultrasound domain. It is also worth to mention that often real loudspeakers shift down to smaller sizes and microphones are equipped with probes to accommodate the measuring instruments to the scaled model and in the same time to avoid appreciable disturbance of the downscaled sound field. A major difficulty aroused in the use of scale models for acoustical measurements is to find a suitable small high performing pair of sound source and detector. In many publications related to this subject, experimentators have often reported such trust in the spark source and the probe microphone [14]. The spark source has three positive features: a satisfactory signal to noise ratio, a good omnidirectionality and an excellent repeatability of the signal. Nowadays, this kind of pulse generator is not of widespread use mainly for its rather high cost and also for its size making it rather cumbersome in practical applications.

#### 3.1. Measurement technique

A technique, sometimes referred to as sweep deconvolution, and developed in the early 1980s for the measurement of impulse responses has shown to be of good reliability, for it has given successful results in many instances. This measurement method consists, as its name suggests, of using a relatively long time duration signal,

a so-called sweep, covering the frequency range of interest. Then, assuming the measurement chain to be linear, a sort of filter is built from the anechoic free field signal sent by the source and collected by the receiver. The impulse response of, say an enclosure, is obtained by simply applying the filter so-obtained to the response of the enclosure to the same sweep used to build the filter. [15,16] This measurement technique has been opted for in this study.

### 3.2. Measurement equipment

When matters come to the sound source, full scale measurements are sometimes easily made by a so-called dodecahedron loudspeaker, an omnidirectional sound source composed of 12 similar speakers distributed evenly on a sphere. On scale models, the non-directional source with adequate power is a major trouble which may be partly overcome by transferring the wave sent by a high performing loudspeaker into a smaller opening. This could be achieved by connecting tightly a hard tube to the loudspeaker. Many papers have been devoted to the study of the radiation of sound from tubes with the early important contribution to the subject by Levine and Schwinger in 1948 [17,18]. The main results of interest concerning the directionality of such a source predict a normalised pressure directivity  $Q(\theta)$  given by: [19,20]

$$[Q(\theta)]^2 = \frac{G(\theta)}{G(0)} = \frac{4 |R|}{\pi (ka \sin \theta)^2} \frac{J_1(ka \sin \theta)}{[J_1^2(ka \sin \theta) + Y_1^2(ka \sin \theta)]^{\frac{1}{2}}} \times \exp \left\{ \frac{2ka \cos \theta}{\pi} \int_0^{ka} \frac{x \operatorname{atan}(-J_1(x)/Y_1(x))}{[x^2 - (ka \sin \theta)^2][ka^2 - x^2]^{\frac{1}{2}}} dx \right\} \quad (17)$$

where

$$|R| = \exp \left\{ -\frac{2ka}{\pi} \int_0^{ka} \frac{\operatorname{atan}(-J_1(x)/Y_1(x))}{x[ka^2 - x^2]^{\frac{1}{2}}} dx \right\} \quad 0 \leq ka < 3.83 \quad (18)$$

the sign  $\int$  means the principal part of the integration defined as: [20]

$$\int_b^c f(x) dx = \lim_{\delta \rightarrow 0} \left[ \int_b^{a-\delta} f(x) dx + \int_{a+\delta}^c f(x) dx \right] \quad \text{if } f(a) \rightarrow \infty \text{ and } b < a < c \quad (19)$$

and  $J_1$ ,  $Y_1$  are, respectively, the Bessel functions of the first and second kind of first order. In the equations above,  $k$  is the wavenumber,  $a$  the inner radius of the cylindrical tube fitted to the transducer and  $\theta$  the angle between the axis of the tube and the line joining the receiver to the acoustic centre  $a$  as illustrated in Fig. 14.

The acoustic centre is the point from which the wave transmitted out of the tube opening diverges spherically. It has been studied first, in a more or less qualitative way in Ref. [21], so its distance from the end of the tube can be approximated by:

$$l \cong -a(0.11 ka - 0.64) \quad 0.5 < ka < 3.5 \quad (20)$$

which shows that the acoustical centre is more off the opening of the tube, the lower is the frequency.

To begin with, a steel tube of length  $L = 25$  cm, and inner radius  $a = 13$  mm has been connected to a tweeter loudspeaker unit. The responses of the loudspeaker both bare and fitted to the tube are illustrated in Fig. 15. As it can be seen, the multiple reflections of the wave in the tube enhance the response of the loudspeaker extended by the tube as compared to the response of the bare loudspeaker, with the resonances corresponding to those of a tube open at one end, i.e.  $kL = (N + 1/2)\pi$ , with  $N$  being some integer.

The study of the directional characteristics of the new source showed good omnidirectionality even for relatively high frequencies.

For the case of the model scale room it is also intended to calculate the cross-correlation between two impulse responses supposed to be the ones at both the listener's ears in the full scale model. Then, instead of a usual microphone for this task,

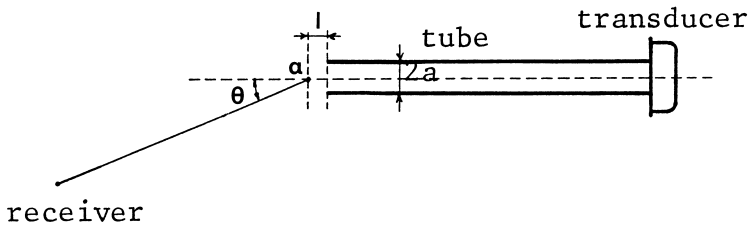


Fig. 14. Illustration of the tube loudspeaker.

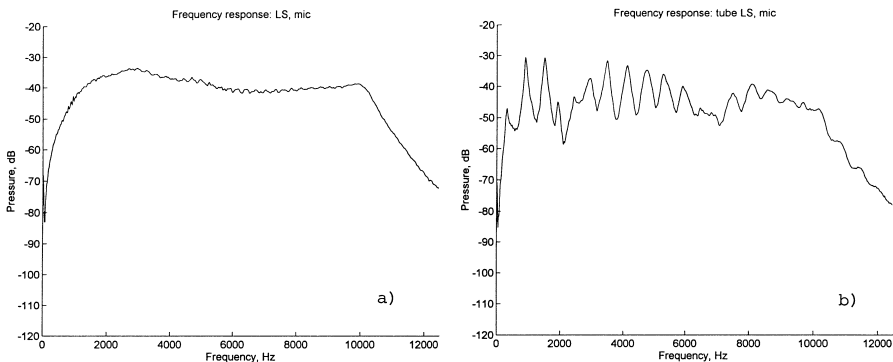


Fig. 15. Response of a small loudspeaker. (a) bare; (b) fitted to a steel tube.

a straight hard probe was used to transmit the pressure perturbations from the measurement point to the sensitive membrane of the microphone. As in the case of the tube loudspeaker, resonances in the frequency response of the probe microphone with length  $l$  occur at  $kl = (n + 1/2) \pi$  where  $k$  is the wavenumber.

When the tubes were mounted on both loudspeaker and microphone, a further precaution had to be taken to avoid the peak responses of both transducers to fall at the same frequencies. Hence, the length  $L$  of the tube fitting on the loudspeaker was chosen so that the inequality:

$$\frac{L}{l} \neq \frac{N + 1/2}{n + 1/2} \quad N, n \text{ integers.} \quad (21)$$

is satisfied at the middle of the working frequency range. This was actually fulfilled by simply setting  $L = l + \lambda/4$  at approximately the middle of the frequency band of interest. The model on which measurements were intended to be performed was a rectangular box with hard walls made of 20 mm thick plywood panels and of size length  $\times$  width  $\times$  height = 200  $\times$  120  $\times$  80 cm<sup>3</sup>. At a scale of 1/12.5 this would represent the room described in the theoretical section. When the room is excited by the broad band sweep, one gets the fir tree-like sweep response typical of a hard room as the complex contribution of all image sources, enhanced by the multiple reflections in the tubes of both loudspeaker and microphone. This is illustrated in Fig. 16.

When the effect of the extra scattering element on the response of the room is sought, then it is simply to measure the impulse response of the room in Fig. 16 with and without the barrier. The results of such measurements with the sweep deconvolution technique is presented in Fig. 17. These measurements were made with the utmost possible care. The model room was lifted off the floor and remained fixed in the anechoic chamber as well as the sound source. The measurement and average of some 10 impulse responses was made for all measurement positions.

In Fig. 17, the positions of, respectively the source and the receiver were at S(0.32,0.6,0.2) and R(1.0,0.6,0.096). One sees from these preliminary results that the effect of the barrier in the room is clearly seen through the extra peaks in the impulse response (pointed by arrows in Fig. 17, right). It should also be mentioned that apart from the extra pulses due to the barrier, the superposition of the impulse responses with and without barrier is almost perfect.

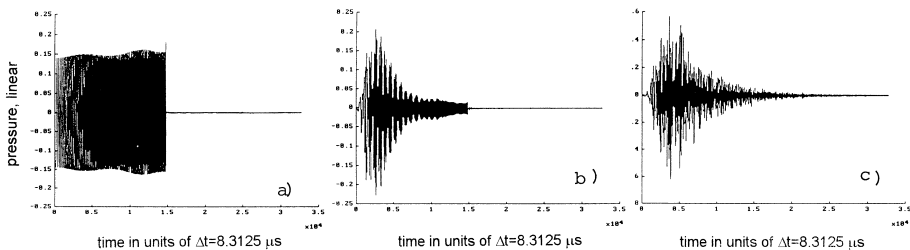


Fig. 16. Measurement of the sweep response of the model room: (a) the signal as generated by the sweep generator; (b) tube LS-probe mic response; (c) sweep response of the model room.

In the model room, nine positions were selected for the evaluation of the IACC as defined in Eqs. (13) and (14), and these values were to be compared to the corresponding calculated ones. On the calculation side, the impulse response was made for a full scale room excited by a narrow triangular pulse. The IACC was not sought for the broad band impulse responses but for the A-filtered ones to come along with the ears' sensitivity. Diffraction around the head of the listener was not taken into consideration. For the model measurements, one has of course to take under consideration the scale factor in the time domain which ought to shorten the time length by a factor of the same order, while values in the frequency domain ought to be stretched in accordance with Eq. (16).

The scaled A-filter was constructed with the help of a YULEWALK filter as a MATLAB subroutine, SIGNAL PROCESSING TOOLBOX [22]. The block diagram of the measurements is shown in Fig. 18. The measurement data were collected and processed in the same computing machine, which hosted the MLSSA circuit board, its software and the MATLAB computing package.

Contrarily to what can be understood from the schematic description in Fig. 18, a single microphone was used for the measurements at both positions not only to avoid disturbing the pressure field but mostly to avoid the problems of calibration and compensation with different microphones. Thus, making two measurements (without and with barrier) for two positions (supposedly the right and left ears) requires a

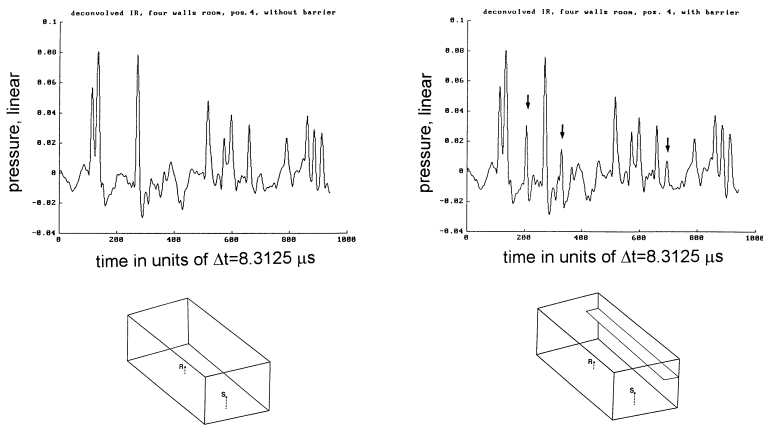


Fig. 17. Impulse responses of the model room (without ceiling and floor in this case): left, without barrier and right, with barrier.

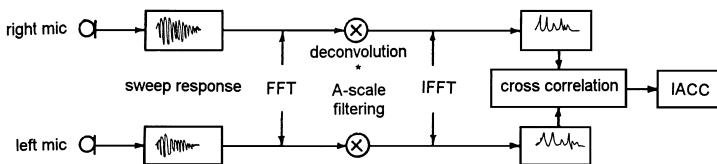


Fig. 18. Block diagram for the measurement of the IACC.

measurement procedure comprising four steps which successively are: take one measurement at a position without barrier and then repeat it after setting the barrier. Then move the microphone to the other position, make a measurement with the barrier and repeat it after removing this latter. The results of the measured values as compared to the calculated ones are summarised in Fig. 19 for the case of a model room with only four side walls.

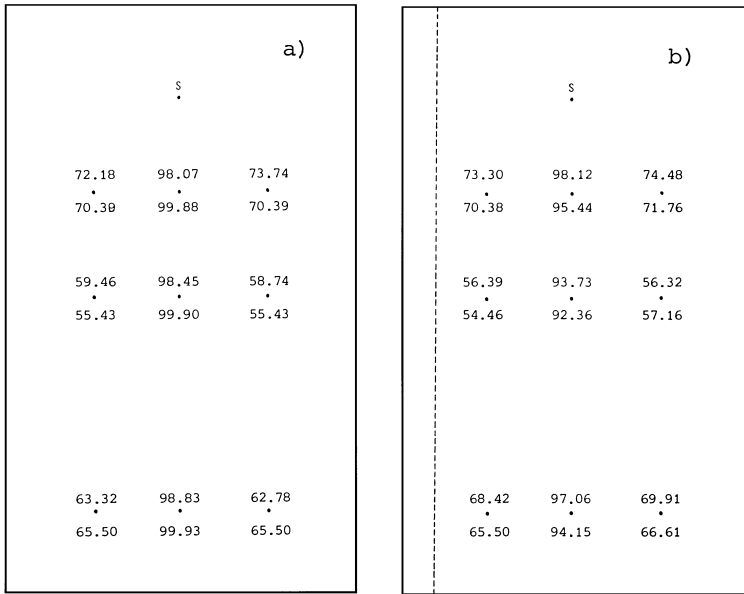


Fig. 19. The IACC as measured (upper values) and calculated (lower values) for a four sidewall room, (a) without barrier, and (b) with barrier.

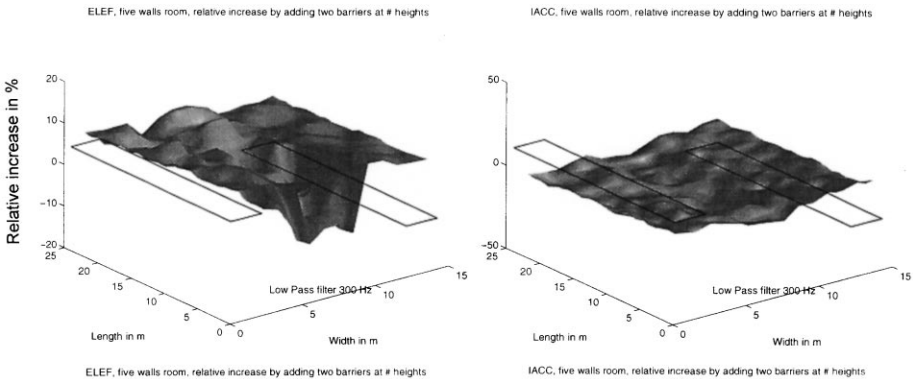


Fig. 20. Relative increase of ELEF, left, and IACC, right, by adding two barriers at different heights. Low pass filtering at 300 Hz. The right and left barriers are placed at respectively, 1/3 and 2/3 of the room height.

Good agreement between predicted and measured values of IACC were also found for the case of a floorless five wall room.

#### 4. Discussion and conclusions

The prediction of some room acoustical parameters was made for a full scale rectangular hard room. Calculations based on the method of images were performed for the real enclosure and measurements based from the impulse response were carried on the corresponding scale model. In this study, option was made for simple geometries of the scattering surfaces for, the first as a simulation of side balconies or decorative motives in the auditoria and second, to combine the image method with some simple diffraction model, preferably in the time domain, to make account of the predicted impulse response of the room. From the convolution of a test signal with the calculated (or measured) impulse response of an auditorium, it is possible to make a subjective evaluation of its acoustical properties [23,24].

The calculations emphasised mainly on two coefficients, the inter-aural cross-correlation coefficient (IACC) and the early lateral energy fraction (ELEF), whereas measurements restricted only to IACC. The changes in values of these quantities may be subjectively assessed in terms of just noticeable differences, jnd, after introduction of the scattering object in the enclosure. The IACC is sensitive to the choice of test signal [25] and the difference limen for Spatial Impression appears to be more sensitive for low frequencies than for a signal with a broad spectrum range [26]. Moreover, jnd have also been found to be dependent on the IACC level; the higher value IACC takes and the more sensitive one becomes in detecting a change in it. Typical reported values of jnd are about 5 and 13% for IACC values of, respectively, 0.8 and 0.6 [27]. Qualitatively, similar results have also been reported from psychological experiments on detecting the differences in the values of the reverberation time  $T$  [1]. The consequences for the ELEF are that with an appropriate choice of the test signal, a high correspondence may be made between IACC and ELEF [25] particularly at frequencies below 1 KHz [28].

In the 1970s, extensive investigations on the factors that could be directly related to the sound quality in rooms led to the result that the cross-correlation of the early portions of the impulse responses at the ears' entrances is closely related to the width and the distance of the sound image. [29,30] The lower the value of this coefficient and the wider seems the image sound source or in other terms the stronger the feeling of envelopment by the sound, a sensation referred to also sometimes as "raumllichkeit" or spatial impression. However, among acousticians, it is not agreed upon which optimal value to attribute to IACC and some say that its preferred value depends strongly on taste [2].

The theoretical calculations of the IACC presented in Fig. 7 can be summarised in what follows: the effect of a single side scattering surface is to break the symmetry of the sound field in the enclosure diminishing thus the values of the IACC especially at the front positions, and this feature is more marked towards higher frequencies and at the positions opposite the scattering element. Adding to the room a similar scattering

element at the opposite wall brings back the geometry to its symmetry and this is translated by higher or at best unchanged values of the IACC. This negative effect of two similar barriers on opposite walls seems to be remedied for by setting the barriers at different heights (see Fig. 20). Regarding the results of Fig. 10, eliminating the absorption of the ceiling and/or the floor results as a rule in a high increment of the IACC values. The opposite trend is found in wide band filtering which confirms the observation that IACC decreases for high pass filtering (wider band) as compared to low pass filtering [2], and that the perception of a wide sound image is even possible in the high frequency range [29].

Using the words of Cremer, during the period of time including the 1970s and 1980s, although the publication of a great number of papers emphasizing the importance of early lateral reflections in auditoria, there is still not a firm consensus among acousticians about among others the required amount of acoustical energy in lateral reflections [31]. In the last years, research has been focused merely on the ELEF and as a conclusion the spatial impression has been confirmed to have two components. The apparent source width, ASW, is influenced by the relative level of early lateral reflections, and the degree of listener envelopment, LEV, which is affected by the level, and angular and temporal distribution of the late arriving energy [32]. The conclusions from this theoretical study are that the effect of a single barrier on a side wall is to increase slightly the ELEF near the opposite wall towards the rear of the room. A second opposite side barrier decreases these values by almost the same amount along the lines running parallel to the barriers at some distance from the walls.

The scattering due to two barriers is found to have antagonist effects on the values of the two acoustical parameters; increasing one where the other one diminishes and vice versa. However, as for the IACC, setting the two opposite barriers at different heights acts beneficially on the ELEF by increasing sensibly its values along the side walls and at the back of the enclosure (Fig. 20). The addition of a ceiling and a floor to the room with four hard side walls acts as to homogenise the distribution of the ELEF values in the room, increasing them especially at the positions near the source and diminishing them elsewhere. Extra median reflections have thus negative effects on the hearing conditions for the rear positions in the room if both IACC and ELEF are considered simultaneously. The behaviour of ELEF for all cases of reflecting surfaces seems independent of frequency as also seen in Fig. 13.

On the measurements' side, the IACC is relatively easy to measure on the scale model. However, the ELEF presents some difficulties. Many experimentators who have measured this quantity use a directive microphone, most often of the pressure gradient type. The impulse response measured by this microphone is then squared (i.e. giving  $p^2 \cos^2(\theta)$ ), integrated from 5 to 80 ms and then normalised to the integrated squared non-directional impulse response. However, this way of measurement is not in accordance with the  $\cos(\theta)$  law given in Eq. (12) which can lead to a wrong assessment of the ELEF value [33].

Lastly, as in reality auditoria are not simple rectangular and hard, and neither are the scattering surfaces always hanging on the sides, thin and of simple shape, this theoretical investigation is naturally insufficient by itself to draw final conclusions

regarding the beneficial use of scattering surfaces in auditoria. It is thus of interest if a further study by simulation, supported by some listening tests in a typical hall could give the decisive answers to for instance the size and placement of side reflectors in rooms for improvement of their acoustics.

## Acknowledgements

The author wishes to express his deep gratitude to Professor Sven G. Lindblad for helping in several ways to the achievement of this work. Sincere thanks are also due to Professor Mendel Kleiner for reading through the text of this paper and for suggesting valuable improvements to the quality of its content.

## References

- [1] Cremer, L., Müller, H. A. and Schultz, T. J., Principles and applications of room acoustics, Vol. I. Applied Science, London, 1982.
- [2] Beranek LL. Concert hall acoustics—1992. *Journal of the Acoustical Society of America* 1992;92: 1–39.
- [3] Kuttruff, H., Room Acoustics, 3rd edn. Elsevier Applied Science, London, 1991.
- [4] Ando, Y., Concert Hall Acoustics. Springer-Verlag, Berlin, 1985.
- [5] Stephenson U. Comparison of the mirror image source method and the sound particle simulation method. *Applied Acoustics* 1990;29:35–72.
- [6] Lee H, Lee BH. An efficient algorithm for the image model technique. *Applied Acoustics* 1988;24:87–115.
- [7] Hammad RNS. Simulation of noise distribution in rectangular rooms by means of computer modelling techniques. *Applied Acoustics* 1988;24:211–228.
- [8] Sommerfeld, A., Optics. Lectures in Theoretical Physics Vol I. Academic Press, New York, 1954.
- [9] Keller JB. Diffraction by an aperture. *Journal of Applied Physics* 1957;28:426–444.
- [10] Kouyoumjian RG, Pathak PH. A uniform geometrical theory of diffraction for an edge in a perfectly conducting surface. *Proceedings of I.E.E.E.* 1974;62:1448–1461.
- [11] Biot MA, Tolstoy I. Formulation of wave propagation in infinite media by normal coordinates with an application to diffraction. *Journal of the Acoustical Society of America* 1957;29:381–391.
- [12] Medwin H. Shadowing by finite noise barriers. *Journal of the Acoustical Society of America* 1981;69:1060–1064.
- [13] Barron M, Marshall AH. Spatial impression due to early lateral reflections in concert halls: derivation of a physical measure. *Journal of Sound and Vibration* 1981;77:211–232.
- [14] Sakurai Y. The early reflections of the impulse response in an auditorium. *Journal of the Acoustical Society of Japan (E)* 1987;8:127–138.
- [15] Berkhout AJ, Boone MM, Kesselman C. Acoustic impulse response measurement: a new technique. *Journal of the Audio Engineering Society* 1984;32:740–746.
- [16] Berkhout AJ. Least-squares inverse filtering and wavelet deconvolution. *Geophysics* 1977;42:1369–1383.
- [17] Levine H, Schwinger J. On the radiation of sound from an unflanged circular pipe. *Physical Review* 1948;73:383–406.
- [18] Johnston GW, Ogimoto K. Sound radiation from a finite unflanged circular duct. *Journal of the Acoustical Society of America* 1980;68:1858–1883.
- [19] Ando Y. Directivity and acoustic centre of the horn loudspeaker. *Acustica* 1968;20:366–369.
- [20] Morse, P. and Feshbach, H., Methods of Theoretical Physics, Vol. I, p. 368, McGraw-Hill, New York, 1953.

- [21] Rayleigh, J. W. S., *The Theory of Sound*. Vol II, sec. 307. Dover, New York, 1945.
- [22] MATLAB, *High Performance Numerical Computation and Visualisation*. The Math Works Inc., Natick, Massachusetts 1994.
- [23] Hojan E, Pösselt C. Subjective evaluation of acoustic properties of concert halls based on their impulse response. *Journal of the Acoustical Society of America* 1990;88:1811–1816.
- [24] Special issue on computer modelling and auralisation of sound fields in rooms, *Applied Acoustics*, 1993, 38, 2–4.
- [25] Barron, M., *Auditorium Acoustics and Architectural Design*. Chapman & Hall, London, 1993.
- [26] Wiliamson RP. Optimisation of variable lateral energy for spatial impression in a hall. *Applied Acoustics* 1989;26:113–134.
- [27] Morimoto M, Lida K, Furue Y. Relation between auditory source width in various sound fields and degree of interaural cross-correlation. *Applied Acoustics* 1993;38:291–301.
- [28] Bradley JS. Comparison of concert hall measurements of spatial impression. *Journal of the Acoustical Society of America* 1994;96:3225–3235.
- [29] Kurozumi K, Ohgushi K. The relationship between the cross correlation coefficient of two channel acoustic signals and sound image quality. *Journal of the Acoustical Society of America* 1983;74:1726–1733.
- [30] Morimoto M, Maekawa Z. Effects of low frequency components on auditory spaciousness. *Acustica* 1988;66:190–196.
- [31] Cremer L. Early lateral reflections in some modern concert halls. *Journal of the Acoustical Society of America* 1989;85:1213–1225.
- [32] Bradley JS, Soulodre GA. The influence of late arriving energy on spatial impression. *Journal of the Acoustical Society of America* 1995;97:2263–2271.
- [33] Kleiner M. A new way of measuring the lateral energy fraction. *Applied Acoustics* 1989;27:321–327.